

Chapter 13

COMPUTED RECONSTRUCTIONS FROM PHASE-ONLY AND AMPLITUDE-ONLY HOLOGRAMS*

John Powers, John Landry, and Glen Wade

*Department of Electrical Engineering
University of California
Santa Barbara, California*

We have analyzed several types of acoustical holograms similar to and including the phase-only hologram suggested by Metherell.¹ The analyses have involved three different diffraction regions: the Fraunhofer, Fresnel, and very-near-field. Each type of hologram studied is characterized by discarding some part of the information present in the wave scattered by the object and recording the portion that is left, thus allowing more efficient use of the recording medium. (For example, in the phase-only hologram the phase information in the scattered wave is retained, but the amplitude information is discarded.) The object investigated in each case was a long slit, thereby confining the analyses to one dimension.

In the cases involving the Fraunhofer region we assumed that the hologram was infinitely wide. Mathematically, the reconstructed image of a slit from a phase-only sideband Fraunhofer hologram of infinite extent is an infinite series of intense lines of light separated by a distance equal to the width of the slit. The two central lines can be regarded as defining the slit edges. The light intensity decreases, but does not drop to zero, between the two central lines. However, it does drop to zero halfway between all other pairs of the intense lines. The reconstructed image from an amplitude-only sideband Fraunhofer hologram bears little resemblance to the slit, although there is some geometric information present.

In the Fresnel and very-near-field regions the analyses were carried out on a digital computer. This was necessitated by having to use the Fresnel-Kirchhoff diffraction integral. Theoretical images were reconstructed for the phase-only, amplitude-only, and conventional holograms. The results indicated that the phase-only process introduces some degree of distortion. The higher spatial frequencies are emphasized and this leads to an exaggeration of edges, corners, etc. This may prove to be useful for many purposes, such as enhancement of object outlines. Also, the phase-only hologram has the advantage of eliminating some of the interfering noise present in the other types of holograms. The amplitude-only holograms seem to have little value in image reconstruction unless the hologram is recorded very close to the object.

Theoretical analysis showed that if the object beam and a bias signal were first added together in conventional fashion, but then only the phase were detected.

*This work supported in part by NIH Grant No. 1. R01 GM 16474-01.

it would be possible to almost duplicate the reconstruction capability of the conventional hologram. The size of the bias signal determines the degree of similarity in the two capabilities. This method has the same advantage as the phase-only process, i.e., only half of the data present must be recorded, and therefore the full dynamic range of the recording medium could be used more efficiently. Reconstruction data obtained from a computer study verified this similarity of image reconstruction.

INTRODUCTION

We have investigated several types of scanned acoustical holograms characterized by some modification of the signal to be recorded. Each such modified signal uses either the phase alone or the amplitude alone of the wave scattered from the object. This type of modification is of interest for its possible application in computer data processing of the holographic information. In recording these modified signals the amount of data present is reduced by about half. This means that the storage requirements and the number of calculations necessary for processing the data can also be reduced.

Intuitively, we would expect that for some objects this reduction of data would cause distortion in the image reconstruction. The images, though distorted, may present enough information about the object (for example, the object's outline) to be useful for many purposes. It can be argued that the most desirable holographic system is one which attains the highest quality of reconstructed image (according to the user's criteria) from the least recorded data. From this point of view it can also be argued that the information capacity of the recording medium is more effectively used by some of these types of holograms than by the conventional acoustical hologram. It is important, therefore, to compare the quality of the reconstructed images from these holograms with that from the conventional hologram.

The various types of holograms considered in this paper are given the following names: the phase-amplitude hologram (i.e., the conventional acoustical hologram), the phase-only hologram, the amplitude-only hologram, and the biased phase-only hologram. Block diagrams, to illustrate how the recorded signals for each are formed, are shown in Figs. 1 and 2. As an example of one of the types of hologram, consider the phase-only hologram (originally proposed by Metherell¹). For this hologram, as shown in Fig. 1(b), only the phase of the scattered wave is measured. This phase is imposed upon a constant-amplitude signal which is then added to an electronic reference signal and recorded on the medium in the usual fashion of scanned acoustical holography.

We have studied the distortion which results from these holographic procedures when some of the available information is deliberately ignored. We have done this by computing the reconstructions of a simple object, an

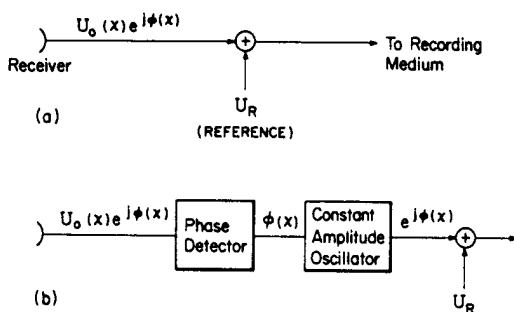


Fig. 1. Block diagrams for the formation of (a) the conventional phase-amplitude hologram, and (b) the phase-only hologram.

infinitely long slit, from each of the above types of hologram. By choosing a long slit, we confine the problem to one dimension. Three different diffraction distances (between object and recording plane) have been investigated: one corresponding to Fraunhofer diffraction, one to Fresnel diffraction, and one to very-near-field diffraction (the latter being where the distance to the recording plane is smaller than that for Fresnel diffraction). In the Fraunhofer case we have mathematically considered an infinitely wide sideband hologram (i.e., with an off-axis reference) and have assumed a slit of arbitrary size. In the Fresnel and very-near-field cases the holographic process was simulated on an IBM 360 Model 65 computer, and for simplicity the holograms were considered to be of the Gabor type (i.e., with an on-axis reference). Some of the results for the phase-only hologram were previously reported,² but are included in this paper for completeness. The object considered in the computer analysis at the distances in the Fresnel and the very-near-field regions was a slit whose width was comparable to the width of the figures

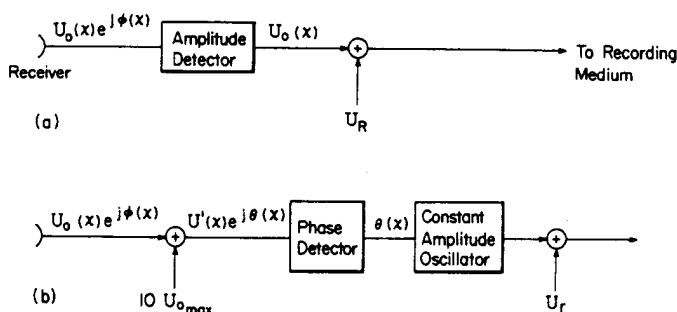


Fig. 2. Block diagrams for the formation of (a) the amplitude-only hologram, and (b) the biased phase-only hologram.

used in experiments performed by Metherell and his colleagues.¹ The slit in question was 0.305 m wide and the insonification wavelength was 0.0186 m (sound in air at 18 kHz). For the Fresnel region the recording plane was assumed to be 4 m wide and was located on-axis a distance of 15 m from the object. For the very near-field region the recording plane was considered to be 2 m wide and located 2 m away from the object.

Because of the different ratios of hologram width to distance, the quality of the images obtained at the two different distances for any of the hologram types are not comparable. It is a characteristic of the Gabor hologram that the spatial frequency generally increases with the distance from the center of the hologram. The recording of fewer fringes because of the geometry implies neglect of the higher spatial frequencies that give sharpness to the edges. This means that our results at the two distances studied on the computer will differ in their basic qualities. Comparison with other types of holograms at the same distance, however, will yield information about the relative quality of the image.

PHASE-AMPLITUDE HOLOGRAM

Fraunhofer Region

The first case considered was that of a conventional hologram, where both the phase and the amplitude of the scattered wave are recorded and used in the reconstruction. Since both phase and amplitude would be measured and stored in a computer, there is no reduction in data for this case. It does, however, provide a basis of comparison for the images from the other methods.

Consider first a single slit in the analytically simple Fraunhofer region. Assume that the slit is of width $2a$ and is placed in a simple holographic system as shown in Fig. 3. We will examine the conventional hologram and its reconstructed real image and then do the same for the other types of holograms. Inspection of the images will illustrate the differences in the various types.

If the distance of the recording medium from the object is great enough so that the diffraction pattern is in the Fraunhofer region, and an off-axis reference beam is used, the recorded hologram is of the sideband Fraunhofer type. Under these circumstances the complex amplitude distribution for the object beam at the holographic plane is given by

$$U_{0,h}(x_h, z_h) e^{-j\omega t} = U_0(x_h) \exp[+j\phi(x_h)] e^{-j\omega t}$$

$$= \left\{ \frac{\exp(jkz_h)}{[j\lambda z_h]^{1/2}} [F\{\text{object}\}]_{f_x = x_h/\lambda z_h} \right\} \exp \left[+j \frac{k}{2z_h} x_h^2 \right] e^{-j\omega t} \quad (1)$$

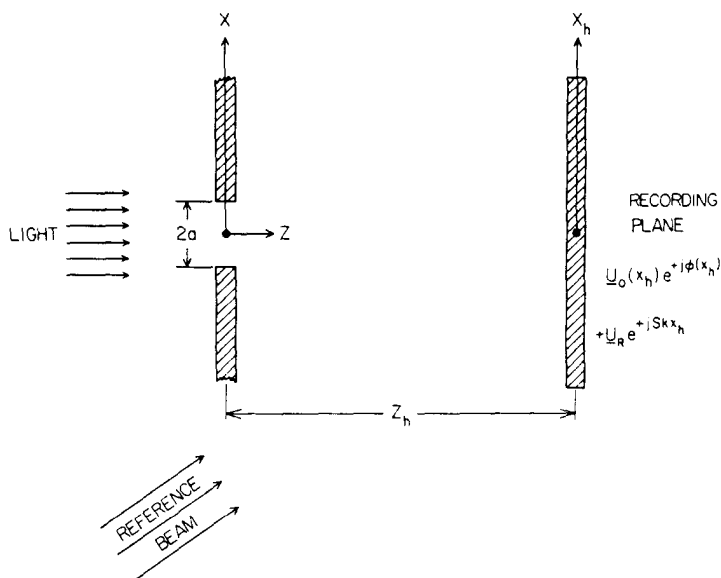


Fig. 3. General recording arrangement for holograms.

where

$$[F\{\text{object}\}]_{f_x = x_h/\lambda z_h}$$

is the spatial Fourier transform of the object with the spatial frequency evaluated at $x_h/\lambda z_h$, and x_h is the distance in the x direction measured at the hologram plane.

For the single slit the complex amplitude distribution is

$$U_o(x_h) \exp[+j\phi(x_h)] = \left\{ \frac{\exp(jkz_h)}{[j\lambda z_h]^{1/2}} 2a \frac{\sin[2\pi(x_h/\lambda z_h)a]}{2\pi(x_h/\lambda z_h)a} \right\} \exp\left[+j\frac{k}{2z_h} x_h^2\right] \quad (2)$$

From this expression it is now easy to identify the amplitude function $U_o(x_h)$ and the phase function $\phi(x_h)$; the factor

$$\left\{ \frac{\exp(jkz_h)}{[j\lambda z_h]^{1/2}} 2a \left| \frac{\sin[2\pi(x_h/\lambda z_h)a]}{2\pi(x_h/\lambda z_h)a} \right| \right\}$$

being the amplitude function and

$$(k^2/2z_h)x_h^2 + f(x_h)$$

the phase function, where $f(x_h)$ has the value $0 (\pm 2n\pi, n \text{ an integer})$ wherever

the function

$$\frac{\sin[2\pi(x_h/\lambda z_h)]a}{2\pi(x_h a/\lambda z_h)}$$

is positive, and the value $\pi (\pm 2n\pi)$ wherever that function is negative.

For a general hologram the complex wave distribution is added to an off-axis wave represented by $U_r \exp(+jSkx_h)$ to form the hologram. Here U_r is a complex constant of position and S is a short-hand notation for the sine of the angle which the reference beam makes with the z axis. The intensity pattern due to the above light is recorded on photographic film and a positive transparency is made. The transmission function of the transparency is proportional to the intensity pattern (for a $\gamma = -2$ film); hence, we have

$$\begin{aligned} t = KI = \frac{1}{2}KUU^* &= \frac{1}{2}K[U_r U_r^* + U_0(x_h)U_0^*(x_h) \\ &+ U_r U_0^*(x_h) \exp\{+j[Skx_h - \phi(x_h)]\} \\ &+ U_r^* U_0(x_h) \exp\{-j[Skx_h - \phi(x_h)]\}] \end{aligned} \quad (3)$$

The reconstruction is performed by illuminating the developed hologram with a planar beam of laser light which is antiparallel to the original reference beam (i.e., by the conjugate of the reference beam). This technique will give a real image which is on-axis and located at the precise original position of the actual object. The beam which then emerges from the hologram is given as follows:

$$\begin{aligned} U_e(x_h, z_h) &= tU_r^* \exp(-jSkx_h) \\ &= \frac{1}{2}K[U_r U_r^* U_r^* \exp(-jSkx_h) \\ &+ U_0(x_h)U_0^*(x_h)U_r^* \exp(-jSkx_h) \\ &+ U_r U_r^* U_0^*(x_h) \exp[-j\phi(x_h)] \\ &+ U_r^* U_r^* U_0(x_h) \exp\{-j[2Skx_h - \phi(x_h)]\}] \end{aligned} \quad (4)$$

Holographic theory provides the interpretation of these terms.³ The first term corresponds to a replica of the reference beam making an angle θ with the axis. The second term represents noise. Because of its dependence on the amplitude function of the scattered wave, we call it the "amplitude noise" term. The third term is the one that gives the real image. As described above, this term is on-axis. The fourth term represents the virtual image. It is found at an angle 2θ off the axis.

Focusing attention on the third term, we realize that if we go a distance $-z_h$ along the z axis from the hologram, we should reproduce a real image of the original object at the origin. Since z_h is large enough to be in the Fraunhofer region, we can find the complex amplitude distribution function at the

image plane by using the Fraunhofer diffraction equation again. Thus, for the slit

$$\begin{aligned}
 U_i(x, 0) &= \left[\frac{KU_r U_r^*}{2} \right] \left\{ \exp \left[+j \frac{k}{2z_h} x^2 \right] \right\} \\
 &\quad \times \int_{-\infty}^{\infty} \frac{\sin(2\pi x_h / \lambda z_h) a}{\pi x_h} \exp \left[-j \frac{k x_h^2}{2z_h} \right] \exp \left[-j 2\pi \frac{x_h}{\lambda z_h} x \right] dx_h \\
 &= \left[\frac{KU_r U_r^*}{2} \right] \left\{ \exp \left[+j \frac{k}{2z_h} x^2 \right] \right\} \\
 &\quad \times \int_{-\infty}^{\infty} \left| \frac{\sin(2\pi x_h / \lambda z_h) a}{\pi x_h} \right| \\
 &\quad \times \exp \left\{ -j \left[\frac{k x_h^2}{2z_h} + f(x_h) \right] - j 2\pi (x_h / \lambda z_h) x \right\} dx_h \quad (5)
 \end{aligned}$$

where $f(x_h)$ is the phase function previously described.

By invoking the Fraunhofer approximation (i.e., the same approximation which allowed the use of the above integral),

$$(k/2z_h)x_h^2 \ll 1, \quad (k/2z_h)x^2 \ll 1$$

we then obtain

$$U_i(x, 0) \approx \frac{1}{2} K U_r U_r^* \begin{cases} = 1 & |x| < a \\ = 0 & |x| > a \end{cases} \quad (6)$$

where the approximation sign reflects the fact that we have applied the Fraunhofer approximation.

This expression for the conventional hologram reconstruction is precisely what we would expect to get by inspecting the third term of Eq. (4). Since that term is a constant times the conjugate of the original object beam, it represents a family of rays having exactly the same ray paths as the original object beam, but with the rays following those paths in the opposite direction. Thus, from Eq. (4) we expect a reconstruction of the original object beam at the object plane.

Hence, the conventional system theoretically gives distortionless image reconstruction of the original object from an infinite sideband Fraunhofer hologram.

Fresnel and Very-Near-Field Regions

For the Gabor hologram used in the computer study the representation of the film transmittance is given by

$$\begin{aligned}
 t &= \frac{1}{2} K U U^* = \frac{1}{2} K \{ U_r U_r^* + U_0(x_h) U_0^*(x_h) \\
 &\quad + U_r U_0^*(x_h) \exp[-j\phi(x_h)] + U_r U_0(x_h) \exp[+j\phi(x_h)] \} \quad (7)
 \end{aligned}$$

[Note that this is the same as Eq. (3) except that the reference beam is on axis and therefore $S = 0$.]

The emerging-beam representation is given by an equation similar to Eq. (4):

$$\begin{aligned} U_e(x_h, z_h) &= tU_r^* \\ &= \frac{1}{2}K\{U_rU_r^*U_r^* + U_0^*(x_h)U_0(x_h)U_r^* \\ &\quad + U_rU_r^*U_0^*(x_h)\exp[-j\phi(x_h)] + U_r^*U_r^*U_0(x_h)\exp[+j\phi(x_h)]\} \quad (8) \end{aligned}$$

Just as in Eq. (4), the first term is a replica of the reference beam, the second represents the noise which we call "amplitude noise," the third gives the real image of the object, and the fourth gives the virtual image.

For a Gabor hologram we note that all terms represent on-axis beam components. This implies that the resulting images will not be spatially separated automatically as in the sideband type of hologram, but that some special means must be used to separate the images. It is possible to use spatial filtering to eliminate the reference beam replica and the virtual image. For computational purposes, therefore, we eliminate these terms mathematically by representing the emerging beam at the hologram plane as

$$U_e(x_h, z_h) = U_0(x_h)U_0^*(x_h)U_r^* + U_r^*U_rU_0^*(x_h)\exp[-j\phi(x_h)] \quad (9)$$

where the reconstruction reference beam U_r^* has been assumed to be anti-parallel to the original reference. Here the emerging beam has terms representing the "amplitude noise" and the real image only. Dividing Eq. (9) by the scaling factor $U_r^*U_r$ and disregarding the overall scale change, we get the emerging-wave representation:

$$U'_e(x_h, z_h) = [U_0(x_h)U_0^*(x_h)/U_r] + U_0^*(x_h)\exp[-j\phi(x_h)] \quad (10)$$

Since our interest was only in the resulting image, Eq. (10) was the logical starting point for the computer calculations. As written, it applies to the phase-amplitude (conventional) hologram, but we can easily modify the equation so that it represents the emerging beam for any of the hologram types being studied. Thus, we can write

$$U'_e(x_h, z_h) = [U'_0(x_h)U_0^*(x_h)/U_r] + U_0^*(x_h)\exp[-j\phi'(x_h)] \quad (11)$$

where $U'_0(x_h)$ and $\exp[j\phi'(x_h)]$ represent the complex wavefront after the required modifications have been imposed to effect the desired type of hologram. The specific modifications for each type will be discussed below.

To use Eq. (10), it was necessary first to calculate $U_0(x_h)\exp[+j\phi(x_h)]$ by applying the Fresnel-Kirchhoff integral to the propagation of the scattered wave from the slit to the hologram plane. This scattered-wave representation [that is, $U'_e(x_h, z_h)$ in Eqs. (10) and (11)] was then put into the Fresnel-

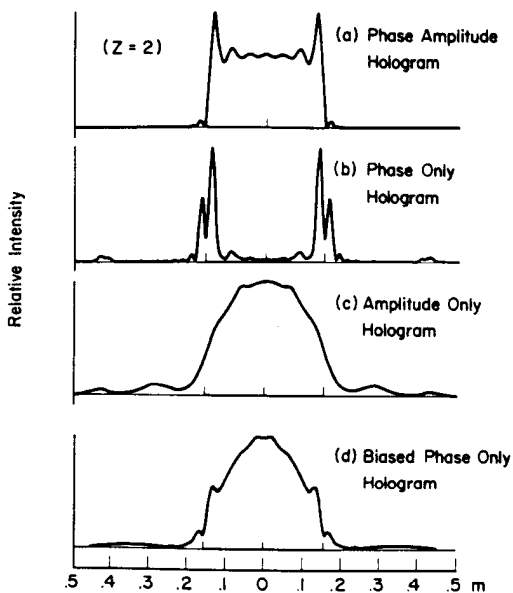


Fig. 4. Image intensity distribution with $z_h = 2.0$ m for the types of hologram noted.

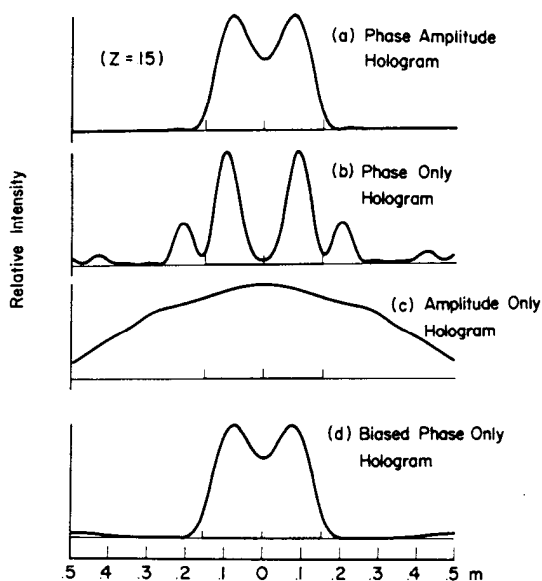


Fig. 5. Image intensity distribution with $z_h = 15.0$ m for the types of hologram noted.

Kirchhoff integral and the complex wave function was computed for propagation to the image plane (a distance equal to that between the object and the hologram plane). The intensity of the image was then calculated and displayed graphically.

The computational procedure was tested by computing images from phase-amplitude (conventional) holograms at the two distances of interest. Following the usual assumption for Gabor holograms, we assume that the reference-beam magnitude is very much greater than the magnitude of the scattered wave. With this assumption the "amplitude noise" term of Eqs. (10) and (11) is negligible compared to the scattered wave. Obtaining the image intensity distribution requires substituting $U'_e(x_h, z_h)$ into the Fresnel-Kirchhoff integral. Note from Eq. (10) that $U'_e(x_h, z_h)$ is the same as the complex conjugate of the previously calculated object wave function $U_o(x_h) \exp[j\phi(x_h)]$. The images obtained at the two distances are shown in Figs. 4(a) and 5(a).

As previously mentioned, the images differ in the number of higher spatial frequencies included in the reconstruction. This constitutes a type of spatial filtering due to the finite size of the recording medium. In spite of this spatial filtering, it is seen that the reconstructions of the slit are quite accurate in the positioning of the edges and in the representation of the intensity across the slit.

PHASE-ONLY HOLOGRAM

Fraunhofer Region

Examining now the case of the phase-only hologram, we proceed as before with the Fraunhofer diffraction integral except that we use only the phase information in the original object beam and not the amplitude information. We thus replace $U_o(x_h)$ in the original expression, Eq. (2), with a constant U_o . Constructing our image as in Eq. (5), we now have

$$U_i(x, 0) = \frac{\exp(+jkz_h) \exp[+j(k/2z_h)x^2] KU_r U_r^*}{[j\lambda z_h]^{1/2}} \frac{2}{2} \times \int_{-\infty}^{\infty} U_o^* \exp \left\{ -j \left[\frac{k}{2z_h} x_h^2 + f(x_h) \right] \right\} \exp \left[-j2\pi \frac{x_h}{\lambda z_h} x \right] dx_h \quad (12)$$

Upon factoring the constant U_o^* out of the expression involving the Fraunhofer approximation and evaluating the Fourier transform of $\exp[-jf(x_h)]$, shown in Fig. 6, we find the result (to within a complex multiplicative constant C):

$$U_i(x, 0) = \frac{C \exp(+jkz_h) KU_r U_r^* \tan(\pi x/2a)}{[j\lambda z_h]^{1/2}} \frac{2}{2} \frac{\pi x/2a}{\pi x/2a} \quad (13)$$

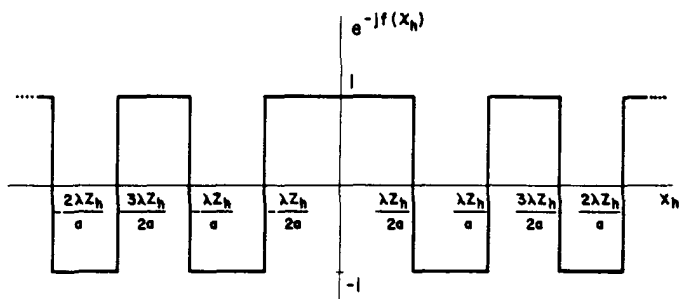


Fig. 6. Graphical representation of the emerging real image term at the hologram plane.

Taking the magnitude squared of this quantity, we obtain the image intensity distribution of Fig. 7.

Here we note that the slit-image reconstruction is an infinite set of intense lines running in the slit direction and located a distance $2a$ apart (i.e., the width of the slit). This repetition of lines is the result of the grating-like structure of the hologram. Since the structure is not strictly periodic, the center of the reconstruction is uniquely located by the nonzero intensity along the center axis half way between the two central lines. These two central lines can be regarded as defining the slit edges in the image. The widths of the other lines decrease with increasing distance away from the central axis. Hence, for this phase-only hologram the reconstructed image

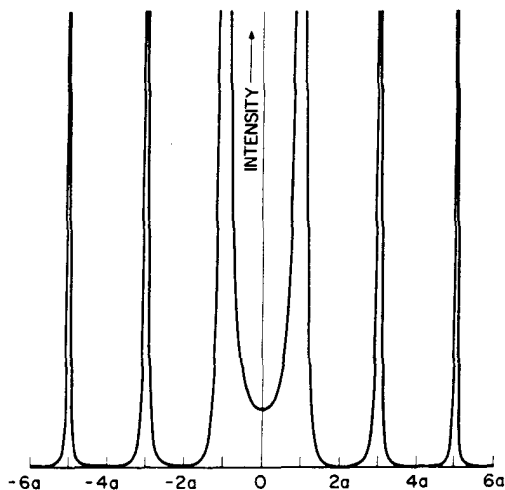


Fig. 7. Reconstructed image intensity distribution from a Fraunhofer phase-only hologram.

of the slit appears with accentuated edges and with an infinite number of periodically distributed lines of light located on both sides of the slit image.

Fresnel and Very-Near-Field Regions

For the case of the phase-only hologram the output of the constant-amplitude oscillator (as shown in Fig. 1b) is assumed to be $\exp[j\phi(x_h)]$ (i.e., the amplitude is constant at unity). Hence, for this case the emerging-wave representation of Eq. (11) becomes

$$U_e(x_h, z_h) = (1/U_r) + 1\{\exp[-j\phi(x_h)]\} \quad (14)$$

It can be noted that the "amplitude-noise" term of Eq. (11) is now constant. This implies that this noise term would be totally removed by the spatial filter in the same fashion as the replica of the reference beam. The removal of the "amplitude-noise" term by spatial filtering represents an advantage over the phase-amplitude (conventional) hologram. With the phase-amplitude hologram we must make the magnitude of the reference beam large to be able to neglect the noise term, since only then would it tend to vanish [see Eq. (10)]. The assumption of large reference beams is not necessary in the phase-only case, thus allowing more generality.

Taking the complex conjugate of the scattered wave function, dividing by its magnitude to normalize the quantity, and putting that into the Fresnel-Kirchhoff integral gives the intensity patterns of Figs. 4(b) and 5(b). Note that the positions of the edges of the slit are slightly misplaced and the intensity across the slit is misrepresented. The edges of the slit are accentuated



Fig. 8. Experimental results from a phase-only hologram showing enhancement of higher spatial frequencies. (Photo courtesy of A. F. Metherell, Douglas Advanced Research Laboratories.)

by the "piling up" of light at their positions. This confirms a distortion seen in photographs (Fig. 8) of reconstructed images made by Metherell and Spinak,⁴ which show the edges of a board as being brightly outlined.

AMPLITUDE-ONLY HOLOGRAM

Fraunhofer Region

In the amplitude-only hologram only amplitude information in the acoustic field is recorded on the medium. Such a hologram can be made experimentally by using an amplitude detector and a constant-phase oscillator as in Fig. 2(a). The use of a square-law (intensity) acoustical sensor would accomplish the same purpose. In fact, the approach is really like holography without a reference beam, although a reference beam was included in our analysis for completeness.

To analyze the Fraunhofer case, we can use the same equations that we developed earlier, with some modifications. In the present case the phase term of Eq. (5) becomes constant, so that we have, for the diffraction equation for the image

$$U_i(x, 0) = \left[\frac{KU_r U_r^*}{2} \right] \exp \left[+j \frac{k}{2z_h} x^2 \right] \times \int_{-\infty}^{\infty} \left| \frac{\sin(2\pi x_h / \lambda z_h) a}{\pi x_h} \right| \exp(-j\phi_0) \exp \left[-j2\pi \left(\frac{x_h}{\lambda z_h} \right) x \right] dx_h \quad (15)$$

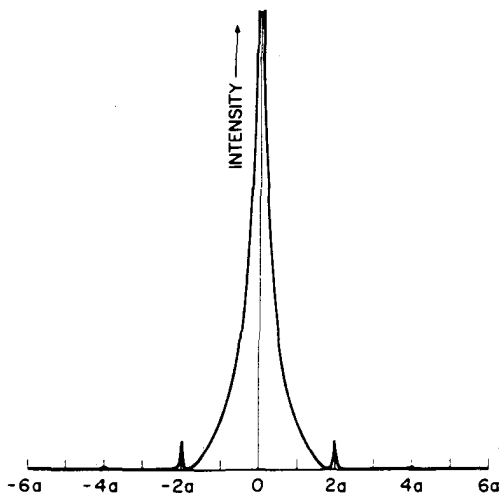


Fig. 9. Reconstructed image intensity distribution from a Fraunhofer amplitude-only hologram.

Performing the indicated transform and finding the magnitude squared, we obtain the intensity distribution of Fig. 9. While some geometric information is present here, the reconstructed image is not of much value in representing the object.

Fresnel and Very-Near-Field Regions

As we have seen, the amplitude-only hologram holds little promise in the Fraunhofer case. It is instructive to consider it in the Fresnel and very-near-field regions also. For this case the modified version of Eq. (11) becomes

$$U'_e(x_h, z_h) = [U_0(x_h)U_0^*(x_h)/U_r] + U_0^*(x_h) \quad (16)$$

When substituted into the Fresnel-Kirchhoff integral the computed images are as displayed in Figs. 4(c) and 5(c). Obviously, as in the Fraunhofer case, image distortion in general is quite high.

However, for the very-near-field case, the image can be quite good. We note from Eq. (16) that when the reference beam is large the emerging wave is approximately the amplitude of the diffracted object wave. For the limiting case in which the hologram is recorded at $z_h = 0$ the diffraction amplitude is just the geometric shadow of the slit. The reconstruction (which is trivial in this case) is then a perfect image of the slit. As the recording distance becomes larger and larger, the diffraction pattern becomes less and less well approximated by the geometric shadow, and eventually the pattern no longer resembles the object. Thus, in the very-near-field we would expect the image to look less and less like that of a slit as we move the recording plane away from the object. In Fig. 4(c) we note that the image obtained resembles the slit, although a deterioration of quality has already set in.

BIASED PHASE-ONLY HOLOGRAM

Theory

As we have seen, the phase-only hologram achieves a decrease in the "amplitude noise" and at the same time gives the advantage of data reduction. One other modification which also does this involves adding a bias term to the signal and then taking the phase of the sum as demonstrated in block diagram form in Fig. 2(b). If the waveform at the receiver is given by $U_0(x_h) \exp[j\phi(x_h)]$, the signal after the addition of an out-of-phase bias signal is

$$\begin{aligned} U' &= U_b \exp(j\phi_0) + U_0(x_h) \exp[j\phi(x_h)] \\ &= U_{b_{RE}} + jU_{b_{Im}} + U_{0_{RE}}(x_h) + jU_{0_{Im}}(x_h) \end{aligned} \quad (17)$$

where $U_{b_{re}}, U_{o_{re}}(x_h)$ and $U_{b_{im}}, U_{o_{im}}(x_h)$ are the real and imaginary parts of the bias and scattered wave. The process of physically detecting the phase of this signal and then producing a unit-amplitude signal that follows this phase can be represented mathematically by the normalization of the input of the phase-detector block of Fig. 2(b). The amplitude of this input from Eq. (17) is

$$|U'| = \{[(U_{b_{re}} + U_{o_{re}}(x_h))^2 + [U_{b_{im}} + U_{o_{im}}(x_h)]^2\}^{1/2} \quad (18)$$

and the normalized waveform which will be recorded at the output is given by

$$\exp[j\theta(x_h)] = \frac{U_b \exp(j\phi_0)}{|U'|} + \frac{U_o(x_h)}{|U'|} \exp[j\phi(x_h)] \quad (19)$$

where $\theta(x_h)$ is the phase angle for the signal consisting of the sum of the bias and the object signals. From this equation it may be seen that if $|U'|$ (which, in general, will vary across the recording plane) could be made to be a constant, then we would have both a replica of a reference beam and of the object beam. Investigating $|U'|$, we note from Eq. (18) that, if the bias term is made very much larger than both the real and imaginary parts of the object beam, then the value of $|U'|$ is approximately a constant, and we have our desired waveform. Under this condition $|U'| \approx U_b$, and we see that we may write Eq. (19) as

$$\exp[j\theta(x_h)] \approx [\exp(j\phi_0)] + \frac{U_o(x_h) \exp[j\phi(x_h)]}{|U'|} \quad (20)$$

We note that all of the information of the scattered wave is contained in the phase angle $\theta(x_h)$.

If a reference signal is then added to the unit-amplitude signal and recorded, the film transmission is

$$\begin{aligned} t &= \frac{K}{2} |U_r + \exp[j\theta(x_h)]|^2 \\ &= \frac{K}{2} \{U_r^2 + 1 + U_r \exp[+j\theta(x_h)] + U_r \exp[-j\theta(x_h)]\} \\ &= \frac{K}{2} \left\{ U_r^2 + 1 + \frac{U_r U_b \exp(j\phi_0)}{|U'|} + U_r \frac{U_o(x_h) \exp[j\phi(x_h)]}{|U'|} \right. \\ &\quad \left. + \frac{U_r U_b \exp(-j\phi_0)}{|U'|} + U_r \frac{U_o^*(x_h)}{|U'|} \exp[-j\phi(x_h)] \right\} \\ &= \frac{K}{2} \left\{ U_r^2 + 1 + \frac{2U_r U_b}{|U'|} \cos \phi_0 \right. \\ &\quad \left. + U_r^* \frac{U_o(x_h)}{|U'|} \exp[j\phi(x_h)] + U_r \frac{U_o^*(x_h)}{|U'|} \exp[-j\phi(x_h)] \right\} \quad (21) \end{aligned}$$

Here the "amplitude-noise" term is decomposed into two parts; one a constant that would be removed by the spatial filter, and the other a term that is approximately a constant across the hologram. Neglecting the reference-beam term and the virtual-image term but including the second of the amplitude-noise terms, the emerging wave becomes, upon reconstruction with a beam of magnitude U_r^{-1}

$$U_e'(x_h, z_h) = \frac{2U_b}{|U'|} \cos \phi_0 + \frac{U_0^*(x_h)}{|U'|} \exp[-j\phi(x_h)] \quad (22)$$

Note that the value of ϕ_0 exerts some control over the size of the effect from the amplitude noise. Assuming that the form of the scattered wave is unknown, it is best to let ϕ_0 be approximately 45° to allow the value of θ to have the maximum range.

Equation (22) is very similar to Eq. (10) for the phase-amplitude hologram. The degree of similarity is determined by how close the quantity $|U'|$ comes to being a constant. Since the equations are so similar, we would expect the images to be of very nearly the same quality. This is true even though the image from the biased phase-only hologram is derived solely from the phase angle $\theta(x_h)$ and all the amplitude information is discarded.

Fraunhofer Region

For the reconstruction of the real image in the Fraunhofer region only, the complex conjugate of the last term of Eq. (19),

$$[U_0(x_h)/|U'| \exp[+j\phi(x_h)]$$

would be put into the Fraunhofer diffraction integral. Here $U_0(x_h)$ and $\phi(x_h)$ are the very same amplitude and phase functions displayed in Eq. (2). To the degree that $|U'|$ approximates a constant, the image obtained by the biased phase-only hologram is an exact duplicate of the image obtained from the phase-amplitude (conventional) hologram, differing only by an amplitude scale factor.

Fresnel and Very-Near-Field Regions

By using Eq. (22) in the Fresnel-Kirchhoff integral and assuming the bias signal to be ten times the maximum value of $U_0(x_h)$, the curves of Figs. 4(d) and 5(d) were obtained. As expected, the results are very similar to those for the phase-amplitude (conventional) hologram. However, some light is present outside of the region of the slit image; also, the edges are less sharply defined. This can be attributed to the variation of amplitude $|U'|$ which, in this case, was not a precise constant across the entire hologram plane.

Although the image is excellent, there are disadvantages in the proposed system which would show up in practice. Since the bias term is larger than the received signal, the measured values of the phase angle $\theta(x_h)$ would be small. The phase detector would have to be able to follow the changes in this angle, however, since these minute changes would contain all of the object information. Hence, the noise of the process must be low.

SUMMARY

It is apparent that real savings in the collection and processing of acoustical holographic data may be made possible by modifying the received signal. As intuitively expected, there are advantages and disadvantages relating to the quality of the reconstructed image for each method. Although our study covered only three possible methods of data reduction for a specific simple object, some general conclusions may nevertheless be drawn.

Because of the simplicity of the Fraunhofer diffraction equation, it is sometimes possible to use Fourier-transform theory to predict the quality of the image from each method for some simple objects (that is, the class of objects whose transforms and inverse transforms may either be found in tables or be calculated).

In the case of the slit, the phase-only hologram proved to contain more geometric information than the amplitude-only hologram, although the phase-only reconstruction was not perfect. The biased phase-only hologram can provide an alternative by using information from both the phase and amplitude while retaining the advantage of requiring only half the data that is contained in the conventional phase-amplitude hologram.

In the Fresnel region and in the very-near-field region the complexity of the Fresnel-Kirchhoff diffraction integral makes it difficult to readily draw such general conclusions. However, a digital computer can be used to calculate the quality of the reconstructions from the standpoint of an arbitrary set of criteria. The biased phase-only hologram theoretically reconstructs a good image, but may be difficult to physically implement because of the small size of the phase angle which must be measured. As explained in the text, the amplitude-only hologram does not image well unless the recording distance is so short that the recorded pattern approximates to a substantial degree the silhouette (or transmission function) of the object. Phase-only holograms, although giving some distortion, may present sufficient information about the object to be highly useful for many purposes. Many types of objects have, in fact, been experimentally reconstructed with little apparent distortion.¹

REFERENCES

1. A. F. Metherell, in *Acoustical Holography*, Vol. 1, (A. F. Metherell, H. M. A. El-Sum, and L. Larmore, eds.) Plenum Press, New York (1969), Chapter 14.
2. G. Wade, J. P. Powers, and C. J. Landry. Image Distortion in Reconstructions from Phase-Only Holograms, Paper H-3, 1968 IEEE Ultrasonics Symposium, New York, September 26, 1968.
3. J. W. Goodman, *Introduction to Fourier Optics*, McGraw-Hill Book Co., New York (1968), Chapter 8.
4. A. F. Metherell and S. Spinak, Acoustical Holography of Nonexistent Wavefronts Detected at a Single Point in Space, *Appl. Phys. Letters* 13(1):22 (1968).